# Structural phase transitions and optical absorption of $LiInSe_2$ under pressure

H. J. Beister, S. Ves,* W. Hönle, and K. Syassen
*Max-Planck-Institut für Festkörperforschung, W-7000 Stuttgart 80, Germany*

G. Kühn
*Sektion Chemie der Universität Leipzig, O-7010 Leipzig, Germany*
(Received 1 October 1990)

We have investigated high-pressure optical and structural properties of the ternary chalcogenide $LiInSe_2$ by optical absorption and reflection and by powder x-ray diffraction. The fundamental absorption edge of $LiInSe_2$ in the ambient-pressure $\beta$-$NaFeO_2$ phase is observed at 2.03 eV. The corresponding band gap is either indirect or pseudodirect. A higher-lying direct absorption edge is observed near 2.9 eV. The variation of these gaps with pressure has been measured up to the first phase transition (4.2 GPa). We propose a tentative assignment of interband transitions based on the band structure of related chalcopyrite compounds and by taking into account the measured pressure coefficients. At 4.2 GPa $LiInSe_2$ transforms from the orthorhombic $\beta$-$NaFeO_2$-type to the cubic NaCl-type structure. At room temperature the NaCl phase is metastable from ambient pressure up to at least 25 GPa. Above 1.5 GPa thermal annealing of the NaCl phase at 210 °C–230 °C causes ordering of the cations and a transition to the $\alpha$-$NaFeO_2$-type structure (rhombohedral; $R\bar{3}m$). Annealing at 210 °C–230 °C below 1 GPa results in a phase transformation from the metastable $\alpha$-$NaFeO_2$ or NaCl phases to the chalcopyrite-type phase (tetragonal; $I\bar{4}2d$). Reflectivity spectra show the high-pressure phases to be nonmetallic.

## I. INTRODUCTION

The ternary chalcogenides $A^{I}B^{III}X_2^{VI}$ ($A$=Cu,Ag; $B$=Al,Ga,In; $X$=S,Se,Te) form tetrahedrally coordinated semiconductors with the potential for technological applications, including solar cells and nonlinear optics. The most common crystal structure among the $A^{I}B^{III}X_2^{VI}$ compounds is isotypic to $CuFeS_2$ (chalcopyrite), which can be considered as a ternary superstructure of the zinc-blende structure. Ternary chalcogenides with tetrahedral coordination are also formed with monovalent alkali-metal cations, where—in contrast to compounds with the noble-metal cations—the bonding and optical properties are not affected by hybridization between cation $d$ and anion $p$ states. In this work we are concerned with the Li-based ($A$=Li) compound $LiInSe_2$. At ambient conditions $LiInSe_2$ crystallizes in the $\beta$-$NaFeO_2$ structure [see Fig. 1(a)], which represents a distorted superstructure of the wurtzite lattice. We report a high-pressure investigation of optical and structural properties of $LiInSe_2$ using optical absorption and *in situ* x-ray powder diffraction measurements.

With respect to the optical properties of $LiInSe_2$ in the ambient-pressure $\beta$-$NaFeO_2$ phase the main questions are related to the nature of the fundamental absorption edge, the spectral dependence of the optical absorption, and the ordering of energy bands in the vicinity of the conduction-band (CB) minimum. From previous luminescence,[1] resistance,[2] absorption,[3] and diffuse reflectance measurements[4] the energy of the fundamental absorption edge of $LiInSe_2$ is not well established and falls into the range of 1.6–2 eV. We have measured the optical absorption for relatively thin single-crystal samples (4 and 60 $\mu$m thickness) in order to characterize the nature of the fundamental absorption regime and to determine the lowest *direct* band gap. By comparing the effect of pressure on absorption features in $LiInSe_2$ to the situation in ternary chalcopyrites[5,6] and related pnictides[7,8] and based on calculated band structures of such materials,[8–13] we propose a tentative assignment of absorption edges in $LiInSe_2$ to interband transitions.

Under pressure the $A^{I}B^{III}X_2^{VI}$ compounds with tetrahedral coordination transform to denser phases with octahedral coordination:[14–17] for $A$=Cu the NaCl-type structure is formed with statistical distribution of $A$ and $B$ cations at the octahedral sites; for $AgGaS_2$ the $\alpha$-$NaFeO_2$ structure is formed, which can be considered as a superstructure of the NaCl lattice arising from cation ordering. The phase-transition pressures for some $A^{I}B^{III}X_2^{VI}$ compounds as well as the energies of the fundamental absorption edges are summarized in Table I. In the case of Li-based ternary chalcogenides ($A$=Li) one observes a similar behavior. $LiInS_2$ also undergoes a phase transition to the NaCl structure. Annealing at 300 °C under pressure leads to the $\alpha$-$NaFeO_2$ structure, which appears to be metastable under ambient conditions.[18] Recent resistivity and x-ray measurements show $LiInSe_2$ to undergo a phase change to the NaCl-type structure at about 4.5 GPa.[19] As for the present x-ray studies of $LiInSe_2$, the primary motivation is to determine the pressure-volume relation over an extended range of pressure and to investigate the effect of thermal treatment on phase changes and on the formation of new metastable phases, while the sample is held under pressure. A preliminary report on the present structural results has been given elsewhere.[20]

 

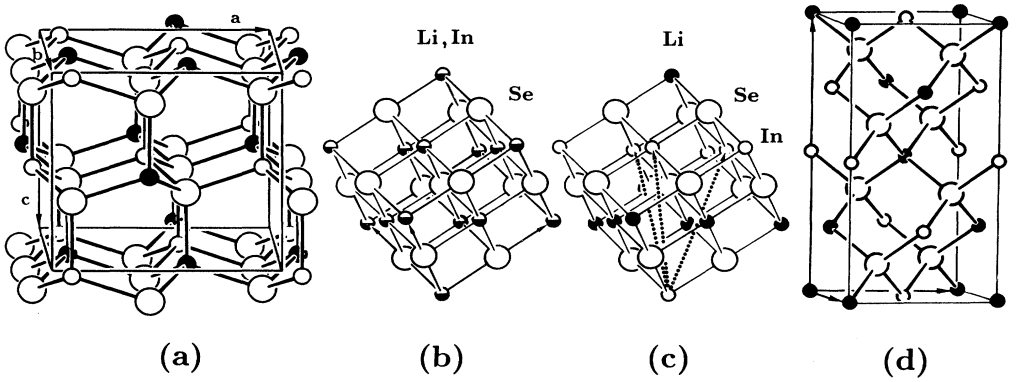


FIG. 1. Crystal structures of $LiInSe_2$ (large open circles, $Se^{2-}$; small open circles, $Li^+$; solid circles, $In^{3+}$). (a) $\beta$-$NaFeO_2$-type structure, stable at ambient pressure. (b) High-pressure NaCl-type structure. Half-filled circles in (b) indicate $Li^+$ and $In^{3+}$ ions in statistical distribution at the cation site. (c) Cation ordering leads to alternating layers of $Li^+$ and $In^{3+}$. Dotted lines indicate the new rhombohedral axes of the $\alpha$-$NaFeO_2$-type structure. (d) $CuFeS_2$-type (chalcopyrite) structure.

A common behavior in tetrahedral III-V semiconductors is that a pressure-induced phase change to a structure with higher coordination goes along with a semiconductor to metal transition. For II-VI compounds the situation is less clear. For a long time the Zn chalcogenides were believed to become metallic at their first high-pressure phase transition to an NaCl-type or related structure, but this is not confirmed by more recent optical investigations.[21] We have measured reflectivity spectra of $LiInSe_2$ under pressure in order to find out if the phase transition to the NaCl-type phase goes along with a semiconductor-to-metal transiton.

## II. EXPERIMENTAL DETAILS

$LiInSe_2$ was synthesized by heating the elements of high purity in sealed quartz ampoules.[22] High-pressure measurements were performed in a gasketed diamond window cell,[23] using the ruby luminescence method for pressure calibration.[24] For optical absorption measurements single-crystal samples were mechanically polished down to two different thicknesses of 4 or 60 $\mu$m, respectively, and cut to dimensions measuring about 100 $\mu$m across. A 4:1 methanol-ethanol mixture served as a pressure medium. Absorption spectra were measured from

TABLE I. Transformation pressures from tetrahedral to octahedral coordination for $A^{I}B^{III}X_2^{VI}$ chalcogenides. Also given are the fundamental energy gaps and the corresponding pressure coefficients of the tetrahedral phases.

| Compound | Structure | $P_{tr}$ (GPa) | HP structure | $E_g$ (eV) | $dE_g/dP$ (meV/GPa) |
|---|---|---|---|---|---|
| $CuGaS_2$ | $CuFeS_2$ | 16[a] | NaCl | 2.40[g] | 34[h] |
| $CuGaSe_2$ | $CuFeS_2$ | 12.5[b] | NaCl | 1.68[g] | |
| $CuGaTe_2$ | $CuFeS_2$ | 8[b] | NaCl | 1.0[i] | |
| $CuInS_2$ | $CuFeS_2$ | | | 1.48[j] | 24[j] |
| $CuInSe_2$ | $CuFeS_2$ | 6[c] | NaCl | 0.98[j] | 30[j] |
| $CuInTe_2$ | $CuFeS_2$ | 2[d] | NaCl | 1.06[k] | |
| $AgGaS_2$ | $CuFeS_2$ | 12[a] | $\alpha$-$NaFeO_2$ | 2.73[g] | 22[h] |
| $AgGaSe_2$ | $CuFeS_2$ | | | 1.81[g,h] | 53[h] |
| $AgInS_2$ | $CuFeS_2$ | 40[d] | NaCl | | |
| $AgInSe_2$ | $CuFeS_2$ | 2.4[c] | NaCl | 1.24[g] | 27[h] |
| $AgInTe_2$ | $CuFeS_2$ | 2[c] | NaCl | 1.12[l] | |
| $LiInS_2$ | $\beta$-$NaFeO_2$ | 1.5[e] | NaCl | 3.26[m] | |
| $LiInSe_2$ | $\beta$-$NaFeO_2$ | 4.1[f] | NaCl | 2.05 | |

[a]Reference 16.
[b]Reference 17.
[c]Reference 15.
[d]Reference 14.
[e]Reference 18.
[f]Reference 19.
[g]Reference 9.
[h]Reference 5.
[i]Reference 41.
[j]Reference 6.
[k]Reference 42.
[l]Reference 43.
[m]Reference 2.

spots of about 30 $\mu$m diameter using a micro-optical system combined with a 0.6-m grating spectrometer and a fast photon counting system. Reflectivity measurements have been performed with the single-crystal sample being in direct contact with the diamond window of the pressure cell. For technical details we refer to Ref. 25. All optical measurements were carried out in the **E⊥a** geometry. Here **E** and **a** denote the vector of the electric field of the incident light and the crystallographic $a$ axis, respectively. For x-ray investigations finely ground $LiInSe_2$ powder was used with paraffin oil as pressure medium. Angle dispersive x-ray data (Mo $K\alpha$ radiation) were collected with a powder diffractometer using a position-sensitive detector. All measurements reported here were performed at room temperature.

## III. RESULTS AND DISCUSSION

### A. Optical absorption

For the single-crystal samples used in absorption measurements the first phase transition is observed at $P_{tr}=4.20(5)$ GPa (increasing pressure), in close agreement with the previous finding ($P_{tr}=4.5$ GPa) from optical observation.[19] At the phase transition even thin samples (thickness 4 $\mu$m), originally with light yellow color, become opaque in the energy region covered by a GaAs photomultiplier ($\hbar\omega \geq 1.5$ eV). After lowering the pressure the crystals remain opaque down to atmospheric pressure.

Absorption spectra of thin samples ($d \sim 4$ $\mu$m) of $LiInSe_2$ at different pressures are shown in Fig. 2(a). The absorption coefficient has been obtained by normalizing the transmission through the sample to the transmission through a clear area next to the sample. The nonvanishing energy-independent background on the low-energy side is attributed to reflectivity losses at the various interfaces. As the photon energy increases the absorption shows a smooth and gradual increase up to $\sim 2.7$ eV, while for higher energies it increases rapidly up to the maximum detectable limit, which is mainly determined by scattered and spuriously transmitted light. The point where the absorption spectra in Fig. 2(a) bend and become flat (see arrow) is taken as the characteristic energy of the absorption edge. This energy does not necessarily match exactly the corresponding band gap, but may be shifted to slightly lower energy due to the stray light limitations mentioned above. This difference, however, is estimated to be quite small (about 0.05 eV) because the obtained values of the absorption coefficient $\alpha$ are of the same order $\sim 2\times 10^4$ cm$^{-1}$ as for direct band gaps in semiconductors with zinc-blende[21,26,27] or chalcopyrite structure.[28,29]

The energy values of the direct absorption edge obtained in the way explained above are plotted as a function of pressure in Fig. 2(b). A least-squares fit to the experimental data gives

$$E_0 = 2.908(2) \text{ eV} ,$$

$$dE_0/dP = 32.8(10) \text{ meV/GPa} .$$

Using a bulk modulus of 43 GPa obtained from x-ray diffraction data (see below), the linear pressure coefficient converts to a gap deformation potential of

$$\frac{-dE_0}{dP} B_0 = -1.4 \text{ eV} .$$

The pressure coefficient (deformation potential) of the 2.9-eV absorption edge in $LiInSe_2$ is considerably smaller than that of direct fundamental gaps ($E_0$ gap, $\Gamma_{15}^v \rightarrow \Gamma_1^c$) in II-VI binaries with zinc-blende structure.[21,30] However, it falls into the range of values observed for direct gaps ($\Gamma_{1\text{ or }6}^v \rightarrow \Gamma_1^c$) in II-VI wurtzite materials[31,32] and for those of In- and Se-based chalcopyrites ($\Gamma_4^v \rightarrow \Gamma_1^c$) given in Table I. Thus the pressure coefficient *as well as* the strength of the absorption edge in $LiInSe_2$ near 2.9 eV compare well with those of II-VI wurtzite semiconductors and ternary chalcopyrites. We therefore interpret the absorption edge as resulting from the lowest direct allowed transition occurring between the valence-band (VB) maximum and conduction-band states at the

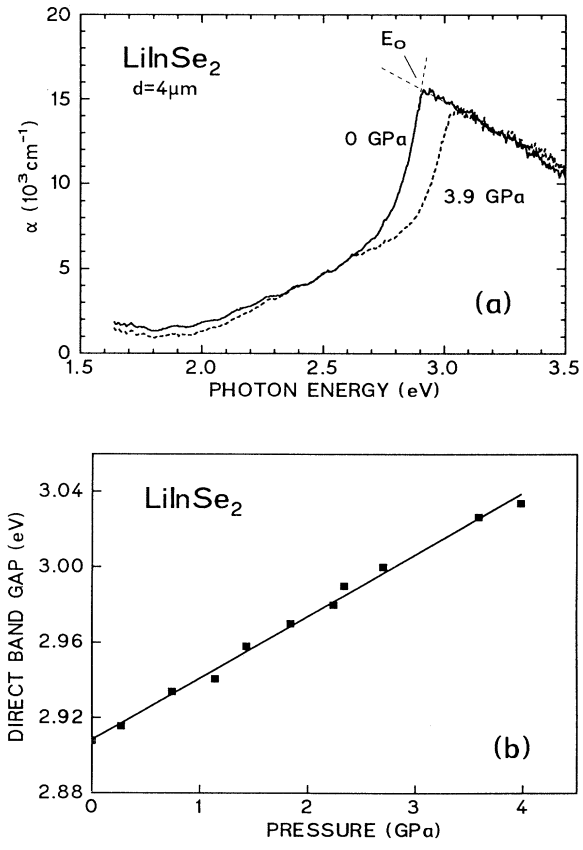


FIG. 2. (a) Absorption spectra of a 4-$\mu$m-thick sample of $LiInSe_2$ in the $\beta$-$NaFeO_2$ structure for two different pressures ($T=300$ K). The arrow indicates the saturation point taken to represent the energy $E_0$ of the direct absorption edge. (b) The energy $E_0$ as a function of pressure. The solid line through the data points is obtained from a linear fit.

Brillouin-zone center, being analogous to the direct fundamental gaps of other tetrahedrally bonded chalcogenides.

Two effects explain the fact that the direct gap value in $LiInSe_2$ is significantly larger compared to, e.g., $CuInSe_2$ (0.98 eV) or CdSe (1.74 eV). First, in the case of $CuInSe_2$ the band gap is quite small due to the hybridization of the Cu $d$ states with the selenium $p$ valence orbitals, which pushes the VB maximum up in energy.[10] Second, the magnitude of the band gap depends on the difference between electronegativities of the constitutents,[33] and the large ionicity of the Li—Se bond[34] is expected to increase the band gap compared to CdSe. A possible consequence of the larger band gap in the case of $LiInSe_2$ is that the CB minimum has a significant admixture of antibonding Se($4p$) states, which would then explain the relatively small pressure coefficient of the direct gap.[10]

Using thicker samples ($d=60$ $\mu$m) the optical density is enhanced, thus facilitating the investigation of the broad absorption below the direct absorption edge in $LiInSe_2$. The corresponding absorption spectra obtained at two different pressures are shown in Fig. 3, where we have plotted the square root of $\alpha$ versus photon energy. The two curves have been adjusted slightly such that they give the same values of $\alpha$ at photon energies of 1.9 and 2.7 eV, assuming that at these energies the sample is completely transparent and absorbing, respectively. In the low-level absorption regime near 2 eV we see hardly any shift in energy as the pressure is increased. In the high-level absorption region a decrease of the absorption coefficient is observed. The latter effect is most likely a consequence of the blue shift of the direct gap at 2.9 eV. A qualitatively similar behavior is observed for the indirect semiconductor GaP under pressure.[35]

We attribute the onset of absorption near 2 eV to the fundamental band gap of $LiInSe_2$. A linear extrapolation of the absorption profile in Fig. 3 below about 2.25 eV yields a gap energy of $E_g=2.03(5)$ eV at ambient pressure. The given uncertainty mainly reflects the scattering of values obtained for extrapolation procedures using other powers of $\alpha$ ($\frac{1}{3}$, $\frac{2}{3}$). Plotting the various powers of $\alpha$ versus photon energy does not allow an unambiguous assignment[36] of the character of the fundamental gap in terms of an allowed or forbidden indirect gap or a forbidden direct gap, respectively. The pressure shift of the gap energy obtained by the extrapolation procedure given above is extremely small ($|dE_g/dP| \leq 5$ meV/GPa).

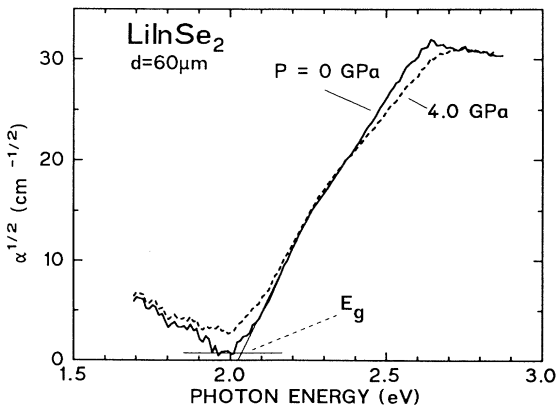


FIG. 3. Square root of the absorption coefficient of a 60-$\mu$m-thick sample of $LiInSe_2$ in the $\mathbf{E}\perp\mathbf{a}$ geometry for two different pressures. The spectra have been adjusted slightly to give the same absorption coefficient in the transparent and saturated regions.

The present value of the fundamental gap at zero pressure agrees to within 0.05 eV with the energy of luminescence bands observed in $LiInSe_2$ at low temperature.[1] The gap values derived from earlier absorption measurements at 300 K (Ref. 3) are lower (1.68–1.88 eV) compared to the present result. This discrepancy can be attributed, at least in part, to the fact that thicker samples were used in previous experiments with an enhanced probability of measuring defect-induced absorption below the fundamental gap.

We offer a qualitative interpretation of the observed absorption behavior *below* 2.8 eV by comparing to related ternary chalcogenides and pnictides crystallizing in the chalcopyrite-type lattice. The ordering of conduction-band states in the ternary noble-metal chalcogenides and also in the heavy cation II-IV-$V_2$ pnictides is such that the $\Gamma_1^c(\Gamma_1)$ state falls below those states ($\Gamma_3^c(X_1), \Gamma_2^c(X_3)$) which appear at the $\Gamma$ point due to folding of the zinc blende into the chalcopyrite Brillouin zone.[7,8,10,11,13] Here the letters in parentheses indicate the originating state in the zinc-blende structure of the binary analogs. Band-structure calculations[9,11] show that in more ionic compounds, the $\Gamma_1^c$ state moves above the folded-in CB states at $\Gamma$. Thus, by analogy we expect pseudodirect optical excitations to appear below the $E_0$ direct gap in $LiInSe_2$, which are derived from indirect transitions in the corresponding wurtzite binary compounds. These transitions are expected to contribute weakly to absorption, since they become allowed only through spin-orbit interaction.[8] Furthermore, CB states at the zone boundary may have energies substantially lower than the $\Gamma_1^c$ state. Thus we expect pseudodirect as well as indirect optical transitions to contribute to the absorption in $LiInSe_2$ at energies below the $E_0$ direct gap. The present experimental data do not allow one to determine unambiguously the character (pseudodirect or indirect) of the absorption in the immediate vicinity of the fundamental gap. Nevertheless, the small pressure coefficient of the fundamental gap in $LiInSe_2$ clearly shows that the corresponding transitions are derived from indirect transitions in the corresponding wurtzite binary compounds.

### B. Structural phase transitions

In powder x-ray diffraction studies we find $LiInSe_2$ to undergo the first-order phase transition from the $\beta$-$NaFeO_2$- (phase I) into the NaCl-type structure (phase II) at $P_{tr}=4.1(3)$ GPa, which is essentially the same value as that obtained from optical observation of single-crystal samples (see above). At ambient temperature the NaCl-type powder pattern is observed up to the maximum pres-

sure of 25 GPa. When decreasing the pressure to zero, the NaCl-type phase remains metastable. The pressure-volume (PV) relations of the $\beta$-$NaFeO_2$- and NaCl-type phases are shown in Fig. 4. The PV data have been fitted by a Murnaghan[37] equation of state $V/V_0 = [(B'/B_0)P+1]^{-1/B'}$, where $B_0$ is the bulk modulus and $B'$ is its pressure derivative. The lines in Fig. 4 refer to the results of the fits. The bulk modulus for the orthorhombic $\beta$-$NaFeO_2$-type phase is

$$B_0 = 42.7(17)\ \text{GPa} \quad \text{with } B' = 4\ \text{(fixed)} .$$

Within experimental uncertainty, the compressibilities are essentially the same for the three axis of the orthorhombic crystal. For the cubic $B1$ phase we obtain

$$B_0 = 52.3(35)\ \text{GPa} \quad \text{and } B' = 4.3(5) .$$

The zero-pressure volume of the cubic high-pressure phase is 84.3(8)% of the orthorhombic normal-pressure volume.

According to an empirical rule of Jayaraman *et al.*[15] the pressures for transitions from tetrahedral to octahedral coordination in $A^{\mathrm{I}}B^{\mathrm{III}}X_2^{\mathrm{VI}}$ compounds increase with decreasing ratio between the averaged cation radius $\bar{r}_{AB}$ and the anion radius $\bar{r}_X$. In particular, the ratio between an averaged cation radius and the anion radius turns out to be an appropriate scaling parameter when comparing $A^{\mathrm{I}}B^{\mathrm{III}}X_2^{\mathrm{IV}}$ compounds with different anions. However, as the data for $LiInSe_2$, $CuInSe_2$ and $AgInSe_2$ in Table II show, this relationship no longer holds for a series of selenides. Instead one observes a systematic increase of the transition pressure with decreasing cation radius difference $\Delta r = |r_A - r_B|$ ($A$=Ag,Li,Cu; $B$=In). Thus, in this special case the radius difference $\Delta r$ appears to be a suitable empirical parameter for estimating the sequence of transition pressures $P_{\mathrm{tr}}$. This observation is somewhat surprising in view of the expected differences in chemical bonding. As discussed in Refs. 22 and 34, the bonding in $LiInSe_2$ can be regarded as being essentially ionic according to the formulation $Li^+(InSe_2)^-$. On the other hand, following Jaffé and Zunger,[12] the strong hybridization between Cu(Ag) $d$ and Se $p$ states in $CuInSe_2$ and $AgInSe_2$ results in a pronounced covalent character of the Cu(Ag)-$X$ bond. This covalent character of the bonding seems to play *no* role in determining the pressure for the transition from tetrahedral to octahedral coordination. In this case the sequence of transition pressures is simply related to radius differences.

TABLE II. Phase-transition pressures and ionic radii of $A^{\mathrm{I}}InSe_2$.

| Compound | Structure | $P_{\mathrm{tr}}$ (GPa) | $\Delta r$ (pm) | $\bar{r}_K/r_{\mathrm{Se}}$ |
|---|---|---|---|---|
| $AgInSe_2$ | $CuFeS_2$ | 2.4 | 45 | 0.523 |
| $LiInSe_2$ | $\beta$-$NaFeO_2$ | 4.1 | 21 | 0.356 |
| $CuInSe_2$ | $CuFeS_2$ | 6.0 | 15 | 0.446 |

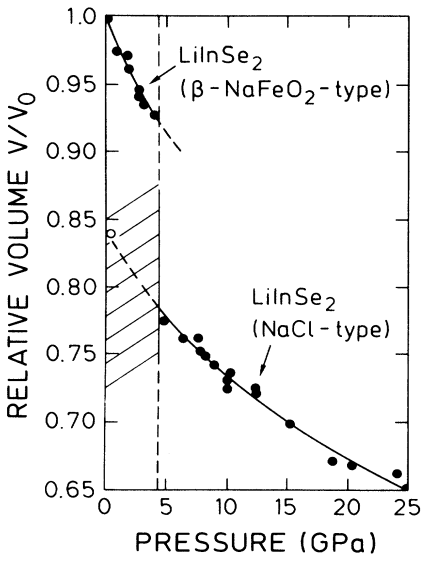


FIG. 4. Pressure-volume relation of $LiInSe_2$. At about 4.2 GPa (increasing pressure) $LiInSe_2$ transforms from tetrahedral to octahedral coordination. The shadowed area shows the region of metastability of the octahedrally coordinated phases. Solid circles refer to increasing pressure, the open circles to decreasing pressure.

The metastable NaCl-type phase obtained by pressure cycling shows further phase transitions upon thermal activation. Heating at $P=1.8$ GPa and $T=210$ °C causes the appearance of additional Bragg reflections in the NaCl-like Debye-Scherrer powder pattern. Figure 5 shows the change of the x-ray powder pattern observed at 1.8 GPa within 11 h heating time.

We have indexed the powder pattern of the new modification (phase III) with respect to a hexagonal crystal system under the assumption that the $\alpha$-$NaFeO_2$-type phase is formed. In this structure Li occupies the Wyckoff 3$a$ site, In the 3$b$ site, and Se occupies the 6$c$ site. In order to refine the positional parameter $z$ of Se, the integrated observed intensities $I_{\mathrm{obs}}$ were transformed into structure factors $F_{\mathrm{obs}}$ according to $F_{\mathrm{obs}} = [(I_{\mathrm{obs}}/n)N_{\mathrm{LPG}}]^{1/2}$, where $n$ is the multiplicity and $N_{\mathrm{LPG}}$ stands for Lorentz, polarization, and geometry factors for the given wavelength and the Debye-Scherrer geometry. The $F_{\mathrm{obs}}$ values were introduced into a single-crystal refinement program SHELX.[38] In the case of coinciding reflections (cf. Table III) the intensities were split according to the ratio of the calculated $F^2_{\mathrm{calc}}$ values as derived from the starting model. After each least-squares refinement the splitting was readjusted. Special care was taken to start with structural models not implying the final result. Within several cycles three parameters [scale factors, $z$(Se), $U_{\mathrm{iso}}$] were refined. Table III lists the observed Bragg reflections of $LiInSe_2$-III and the observed and calculated structure factors. For the positional parameter of Se we obtain $z=0.2500(9)$. The common thermal parameter $U_{\mathrm{iso}}$ has been refined to 107(82) pm$^2$. The final residual factor reached was $R=0.069$ ($R = |F_{\mathrm{obs}} - F_{\mathrm{calc}}|/|F_{\mathrm{obs}}|$). The results show that the

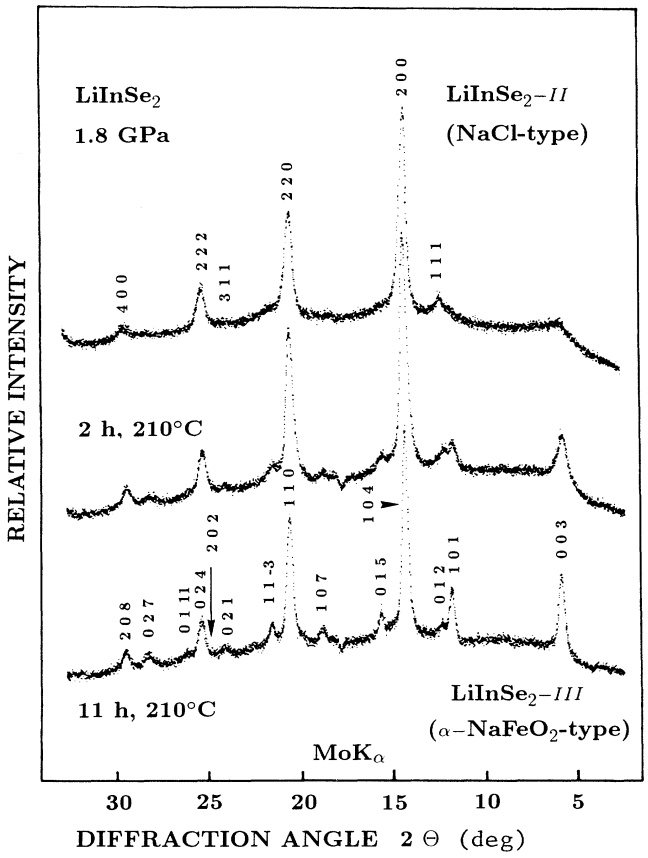


FIG. 5. Change of the Debye-Scherrer pattern of $LiInSe_2$ during thermal annealing at 1.8 GPa. The starting material was the metastable NaCl-type phase.

TABLE III. List of observed $d$ values (in pm), peak intensities, and observed and calculated structure factors for the ordered octahedral phase of $LiInSe_2$ (phase III, $\alpha$-$NaFeO_2$-type).

| $d_{obs}$ | $h$ | $k$ | $l$ | $I_{obs}$ | $F_{obs}$ | $F_{calc}$ |
|---|---|---|---|---|---|---|
| 641.7 | 0 | 0 | 3 | 550 | 15.0 | 13.1 |
| 331.8 | 1 | 0 | 1 | 267 | 117.5 | 116.5 |
| 317.1 | 0 | 1 | 2 | 66 | 61.0 | 42.9 |
| 275.7 | 1 | 0 | 4 | 1000 | 274.5 | 281.4 |
| 253.7 | 0 | 1 | 5 | 141 | 112.4 | 107.5 |
| 212.6 | 1 | 0 | 7 | 78 | 100.1 | 100.2 |
| 194.8 | 0 | 1 | 8 | 689 | 230.8 | 245.4 |
| | 1 | 1 | 0 | | 230.8 | 244.5 |
| 185.9 | 1 | 1 | 3 | 108 | 96.0 | 93.6 |
| | 1 | 1 | $\bar{3}$ | | | |
| 167.5 | 0 | 2 | 1 | 33 | 83.8 | 88.1 |
| 159.1 | 0 | 2 | 4 | 251 | 244.7 | 218.5 |
| 154.4 | 0 | 1 | 11 | 26 | 80.7 | 83.8 |
| 143.7 | 0 | 2 | 7 | 84 | 91.2 | 79.1 |
| | 1 | 1 | 9 | | 91.2 | 79.2 |
| | 1 | 1 | $\bar{9}$ | | | |
| 137.9 | 2 | 0 | 8 | 108 | 187.1 | 198.2 |

bond distances $d$(LI-Se) and $d$(In-Se) in phase III are the same within standard deviations. We note that already in the $\beta$-$NaFeO_2$-type structure these bond distances differ by 3 pm only.

The crystal structure of $LiInSe_2$-III consists of a fcc packing of the anions, with all the octahedral holes filled by the cations in an ordered way (NaCl superstructure). It can also be regarded as a filled-up $CdCl_2$ structure with alternating Li and In planes in subsequent cation layers along the rhombohedral axis. The crystal structure of $LiInSe_2$-III is shown in Fig. 1(c), with the new rhombohedral axes indicated by dotted lines.

Samples transformed to the $\alpha$-$NaFeO_2$ phase at low pressure have been exposed again to pressures up to 18 GPa. The $\alpha$-$NaFeO_2$-type structure was found to be stable under such conditions, but a strong damping of the (003) Bragg reflection indicates a distortion of the lattice. The same result has been obtained by thermal treatment of the disordered NaCl-type structure at pressures above 10 GPa. Transformation to the $\alpha$-$NaFeO_2$ structure takes place even at these fairly high pressures, but the relative intensity of the (003) reflection is always less compared to the intensity at lower pressures. A similar refinement as above has been performed with the intensity data from a measurement at 12.2 GPa after heating the sample at 230 °C for 4.5 h. The results are $R=0.13$, $z$(Se)$=0.252(2)$, the $U$ value due to the small degree of overestimation (12 $hkl$ values, 3 parameter) is nonpositive definite. From this refinement the tendency is clear that, under the given experimental conditions, the octahedra become nonequivalent with slightly different bond lengths of $d$(Li-Se)$=261(2)$ pm and $d$(In-Se)$=265(2)$ pm. The fact that the transformation from the NaCl-type to the $\alpha$-$NaFeO_2$-type structure is observed even at pressures above 10 GPa shows that the disordered NaCl-type high-pressure phase is a metastable polytype.

Starting with the disordered NaCl-type phase or the $\alpha$-$NaFeO_2$ phase we have also performed annealing experiments close to zero pressure. Heating at $T=210$ °C–230 °C for more than 10 h while the pressure is held at $P \leq 1.1$ GPa leads to a new x-ray powder pattern which can be indexed as tetragonal. From the ratio $c/a=2.034$ ($p=0.3$ GPa) and the indices and intensities of the Bragg reflections we infer that $LiInSe_2$-II and -III transform to the chalcopyrite-type phase $LiInSe_2$-IV. The color of this phase is red. At pressures of about 4 GPa this tetragonal phase transforms again to the NaCl-type phase, changing the color from red to black. A chalcopyrite-type phase has been observed earlier by electron diffraction for thin epitaxial layers of $LiInSe_2$ grown on a GaAs substrate.[39] The reported $c/a$ ratio was about 1.9, which indicates a stronger distortion of the epitaxially grown chalcopyrite lattice, compared to the material obtained in the present experiments.

The sequence of phase transitions in $LiInSe_2$, as induced by the application of pressure and in combination with thermal annealing, is illustrated by the sequence of structures shown in Figs. 1(a)–1(d). The crystallographic details of the various phases of $LiInSe_2$ are summarized in Table IV.

TABLE IV. Summary of structural data for the different phases of $LiInSe_2$ ($P$ is the pressure, $V$ is the unit cell volume, and $Z$ is the number of formula units in the unit cell).

| Phase | Structure | Space group | $P$ (GPa) | Lattice constant (pm) | $V/Z \times 10^{-6}$ $(pm)^3$ |
|---|---|---|---|---|---|
| $LiInSe_2$-I | $\beta$-$NaFeO_2$ | $Pna2_1$ | 0 | $a=718.3(2)$<br>$b=839.8(3)$<br>$c=678.1(2)$ | 102.3 |
| $LiInSe_2$-II | NaCl | $Fm\bar{3}m$ | 4.1 | $a=544.4(3)$ | 80.7 |
| $LiInSe_2$-III | $\alpha$-$NaFeO_2$ | $R\bar{3}m$ | 1.8 | $a=388.7(3)$<br>$c=1925.4(13)$ | 84.0 |
| $LiInSe_2$-IV | $CuFeS_2$ | $I\bar{4}2d$ | 0.27 | $a=580.7(8)$<br>$c=1181.0(31)$ | 99.6 |

### C. Reflectivity under pressure

Optical reflectivity spectra of $LiInSe_2$ taken below and above the first phase transition are shown in Fig. 6. Spectra measured below the phase transition exhibit an edge at the fundamental gap energy $E_g$. This is just an artifact which arises because for photon energies below $E_g$ intensity is reflected at the back surface of the sample. In the spectra of the $\beta$-$NaFeO_2$ phase one clearly observes a peak near 2.9 eV, which shifts to higher energy with increasing pressure. Obviously, this peak is due to the direct optical transition at the $\Gamma$ point. Thus the optical reflectivity spectra are consistent with the interpretation of the absorption spectra given above.

The reflectivity spectrum measured above the first phase transition is similar to that of the low-pressure phase except for the absence of any pronounced feature which could be attributed to interband absorption edges. The important observation is that the reflectivity of the high-pressure phase does not show evidence for free-carrier behavior, i.e., no Drude-like increase of the reflectivity in the near-infrared spectal range. This behavior is observed for pressures up to 25 GPa. Thus, from the reflectivity spectra we infer that $LiInSe_2$ remains semiconducting after the first high-pressure phase transition.

Finally, we note that at about 10 GPa the layered semiconducting compound InSe also undergoes a phase transition to the NaCl-type lattice.[40] InSe in the $B1$ phase is metallic as evidenced by optical reflectivity measurements. Thus the dilution of the In concentration by Li in the cation sublattice of the $B1$ structure not only results in a 10% decrease of the specific volume but also in a shift from metallic to semiconducting behavior.

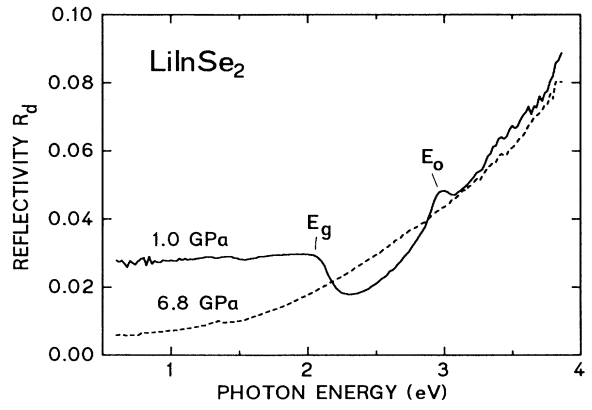


FIG. 6. Reflectivity spectra of $LiInSe_2$ measured below (1.0 GPa) and above (6.8 GPa) the pressure-induced phase transition from the $\beta$-$NaFeO_2$ to the disordered NaCl-type phase.

## IV. CONCLUSIONS

The optical absorption of the ternary chalcogenide $LiInSe_2$ in the low-pressure $\beta$-$NaFeO_2$ phase, measured for two different sample thicknesses and for pressures up to the first phase transition (4.2 GPa), reveals that (i) the direct optical gap of $LiInSe_2$ corresponding to the fundamental $\Gamma_6^v \rightarrow \Gamma_1^c$ gap in the II-VI wurtzite analogs is quite large (2.9 eV) and (ii) the fundamental gap is located at much lower energy (2.03 eV). The optical absorption within about 0.8 eV above the fundamental gap is attributed to a combination of indirect transitions and pseudodirect transitions, the latter originating from the folding of the wurtzite Brillouin zone into that of the $\beta$-$NaFeO_2$ structure. A band-structure calculation of $LiInSe_2$ in the $\beta$-$NaFeO_2$ phase would be quite helpful in clarifying the ordering in energy of conduction-band states.

Using powder x-ray diffraction we have obtained the pressure-volume relation of $LiInSe_2$ up to 25 GPa. The first phase transition from the $\beta$-$NaFeO_2$ to the NaCl-type structure at 4.2 GPa is coupled with a change of the distorted wurtzitelike hexagonal stacking of the anion lattice to a close-packed cubic sequence. After the breakdown of the $\beta$-$NaFeO_2$ structure the cations are randomly distributed over the octahedral sites of the lattice. This disordered NaCl-type phase remains metastable upon releasing the pressure. Thermal annealing of the NaCl phase results in the formation of two new structures. At pressures above 1.5 GPa we observe an ordering of the cations with the cubic close-packed anion stacking of the NaCl lattice being preserved. This leads to the $\alpha$-$NaFeO_2$-type structure, which is observed up to at least 18 GPa. High pressure leads to a reversible distortion of the $\alpha$-$NaFeO_2$ structure. The Li—Se bond is found to be more compressible than the In—Se bond. Annealing of the $\alpha$-$NaFeO_2$ or NaCl phases at pressures below 1.1 GPa yields a tetrahedrally coordinated com-

pound isotypic to $CuFeS_2$ (chalcopyrite type), where the anion stacking sequence still is cubic, but the cations now occupy the tetrahedral sites within the anion lattice. It appears that the formation of the NaCl- and $\alpha$-$NaFeO_2$-type high-pressure phases favor, upon back-transformation to tetrahedral coordination, the zinc-blende-like over the wurtzitelike anion stacking.


## ACKNOWLEDGMENTS

We thank S. Heymann for help with the reflectivity measurements and D. Oppermann for sample preparation. One of us (S.V.) gratefully acknowledges financial support from the Max-Planck-Gesellschaft.



*Permanent address: Physics Department, Aristotles University, Thessaloniki, Greece.

[1]K. Kuriyama and Y. Igarashi, J. Appl. Phys. **56**, 1884 (1984); T. Kamijoh, T. Nozaki, and K. Kurijama, Nuovo Cimento **20**, 2089 (1983).

[2]T. Kamijoh and K. Kuriyama, J. Appl. Phys. **52**, 1102 (1981).

[3]T. Kamijoh and K. Kuriyama, J. Cryst. Growth **51**, 6 (1981); W. Hörig, H. Neumann, and G. Kühn, Phys. Status Solidi B **121**, K55 (1984); S. Mitaray, G. Kühn, B. Schumann, A. Tempel, W. Hörig, and H. Neumann, Thin Solid Films **135**, 251 (1986).

[4]I. Smith and G. W. Lowe, J. Appl. Phys. **66**, 5102 (1989).

[5]A. Jayaraman, V. Narayanamurty, H. M. Kasper, M. A. Chin, and R. G. Maines, Phys. Rev. B **14**, 3516 (1976).

[6]J. González and C. Rincón, J. Appl. Phys. **65**, 2031 (1989).

[7]R. Bendorius, V. D. Prochukan, and A. Sileika, Phys. Status Solidi B **53**, 745 (1972).

[8]A. Shileika, Surf. Sci. **37**, 730 (1973).

[9]I. L. Shay and I. H. Wernick, *Ternary Chalcopyrite Semiconductors: Growth, Electronic Properties and Applications* (Pergamon, Oxford, 1974).

[10]J. E. Jaffé and A. Zunger, Phys. Rev. B **28**, 5822 (1983).

[11]J. E. Jaffé and A. Zunger, Phys. Rev. B **30**, 741 (1984).

[12]J. E. Jaffé and A. Zunger, Phys. Rev. B **29**, 1882 (1984).

[13]M. L. Cohen and J. R. Chelikowsky, in *Electronic Structure and Optical Properties of Solids,* Springer Series in Solid State Sciences, Vol. 75 (Springer, Berlin, 1988).

[14]K. J. Range, G. Engert, and A. Weiss, Solid State Commun. **7**, 1749 (1969).

[15]A. Jayaraman, P. D. Dernier, H. M. Kasper, and R. G. Maines, High Temp. High Press. **9**, 97 (1977).

[16]A. Werner, H. D. Hochheimer, and A. Jayaraman, Phys. Rev. B **23**, 3836 (1981).

[17]A. Kraft, G. Kühn, and W. Möller, Z. Anorg. Allg. Chem. **504**, 155 (1983).

[18]C. J. M. Rooymans, in *Reactivity of Solids,* edited by G. M. Schwab (Elsevier, Amsterdam, 1974), pp. 100–109.

[19]B. Greuling, Cryst. Res. Technol. **22**, K27 (1987).

[20]H. J. Beister, W. Hönle, K. Syassen, and G. Kühn, High Press. Res. **4**, 360 (1990).

[21]S. Ves, U. Schwarz, N. E. Christensen, K. Syassen, and M. Cardona, Phys. Rev. B **42**, 9113 (1990), and references therein.

[22]W. Hönle, G. Kühn, and H. Neumann, Z. Anorg. Allg. Chem. **543**, 161 (1986).

[23]For a review, see A. Jayaraman, Rev. Mod. Phys. **55**, 55 (1983).

[24]G. J. Piermarini, S. Block, J. D. Barnett, and R. A. Forman, J. Appl. Phys. **46**, 2774 (1975); H. K. Mao, J. Xu, and P. M. Bell, J. Geophys. Res. **91**, 4673 (1986).

[25]K. Syassen and R. Sonnenschein, Rev. Sci. Intrum. **53**, 644 (1982).

[26]*Numerical Data and Functional Relationships in Science and Technology,* edited by O. Madelung, H. Weiss, and M. Schulz, Landolt-Börnstein, New Series, Vol. 17b (Springer, Berlin, 1982).

[27]A. Goñi, K. Strössner, K. Syassen, and M. Cardona, Phys. Rev. B **36**, 1581 (1987).

[28]D. Haneman, Crit. Rev. Solid State Mater. Sci. **14**, 377 (1988), and references therein.

[29]G. Kühn and H. Neumann, Z. Chem. **27**, 197 (1987), and references therein.

[30]See also S. Ves, K. Strössner, N. E. Christensen, C. K. Kim, and M. Cardona, Solid State Commun. **56**, 479 (1985); K. Strössner, S. Ves, C. K. Kim, and M. Cardona, *ibid.* **61**, 2755 (1987).

[31]Measured pressure coefficients (in meV/GPa) in II-VI wurtzite compounds are CdSe=37,58 [A.L. Edwards and H. Drickamer, Phys. Rev. **122**, 1449 (1961); J. R. Mei and V. Lemos, Solid State Commun. **52**, 785 (1984)]; CdS=46,45 [B. Battlogg, A. Jayaraman, J. E. Van Cleve, and R. G. Maines, Phys. Rev. B **27**, 3920 (1983); U. Venkatewaran and M. Chandrasekhar, *ibid.* **31**, 1219 (1985)].

[32]We use the nonrelativistic notation (spin-orbit interaction neglected). For the wurtzite structure the Rashba classification has been used, which, compared to the Koster notation, causes an interchange of the $\Gamma_6$ and $\Gamma_5$ states.

[33]V. P. Gupta, V. K. Srivastava, and P. N. L. Gupta, J. Phys. Chem. Solids **42**, 1079 (1981).

[34]H. Neumann, Cryst. Res. Technol. **21** 1207 (1986), and references therein.

[35]A. Goñi, K. Syassen, K. Strössner, and M. Cardona, Phys. Rev. B **39**, 3178 (1989).

[36]O. Madelung, *Solid State Theory* (Springer, Berlin, 1978).

[37]F. D. Murnaghan, Proc. Natl. Acad. Sci. U.S.A. **30**, 244 (1944).

[38]G. M. Sheldrick, Structure Determination System SHELX, Version 3.0, 1985 (unpublished).

[39]A. Tempel, B. Schumann, S. Mitary, and G. Kühn, Cryst. Res. Technol. **21**, 1429 (1986).

[40]U. Schwarz, A. R. Goñi, K. Syassen, A. Cantarero, and A. Chevy, High Press. Res. (to be published).

[41]M. Neumann *et al.*, Thin Solid Films **61**, 13 (1979).

[42]M. J. Twaites, R. D. Tamlinson, and M. J. Hampshire, Solid State Commun. **23**, 905 (1977).

[43]V. M. Mirgorodskii, S. J. Radautsan, and A. E. Tsurkon, Opt. Spectrosk. **39**, 519 (1975) [Opt. Spectrosk. (USSR) **39**, 291 (1975)].